

# Understanding the Modulation of $\alpha$ -Synuclein Fibrillation by *N*-Acetyl Aspartate: A Brain Metabolite

Tanzeel Khan, Rashid Waseem, Mohammad Shahid, Jaoud Ansari, Md. Imtaiyaz Hassan, Anas Shamsi,\* and Asimul Islam\*

Cite This: *ACS Omega* 2024, 9, 12262–12271

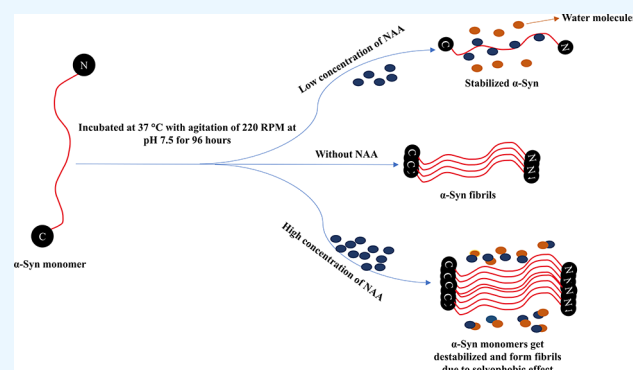
Read Online

ACCESS |

Metrics & More

Article Recommendations

**ABSTRACT:**  $\alpha$ -Synuclein ( $\alpha$ -Syn) fibrillation is a prominent contributor to neuronal deterioration and plays a significant role in the advancement of Parkinson's Disease (PD). Considering this, the exploration of novel compounds that can inhibit or modulate the aggregation of  $\alpha$ -Syn is a topic of significant research. This study, for the first time, elucidated the effect of *N*-acetyl aspartate (NAA), a brain osmolyte, on  $\alpha$ -Syn aggregation using spectroscopic and microscopic approaches. Thioflavin T (ThT) assay revealed that a lower concentration of NAA inhibits  $\alpha$ -Syn aggregation, whereas higher concentrations of NAA accelerate the aggregation. Further, this paradoxical effect of NAA was complemented by ANS, RLS, and the turbidity assay. The secondary structure transition was more pronounced at higher concentrations of NAA by circular dichroism, corroborating the fluorescence spectroscopic observations. Confocal microscopy also confirmed the paradoxical effect of NAA on  $\alpha$ -Syn aggregation. Interaction studies including fluorescence quenching and molecular docking were employed to determine the binding affinity and critical residues involved in the  $\alpha$ -Syn-NAA interaction. The explanation for this paradoxical nature of NAA could be a solvophobic effect. The results offer a profound understanding of the modulatory mechanism of  $\alpha$ -Syn aggregation by NAA, thereby suggesting the potential role of NAA at lower concentrations in therapeutics against  $\alpha$ -Syn aggregation-related disorders.



## 1. INTRODUCTION

Parkinson's disease (PD) is a multifaceted and progressive neurodegenerative disorder that is distinguished by the presence of tremors, rigidity, bradykinesia, and postural instability.<sup>1</sup> The advancement of PD significantly reduces the quality of life and impairs general performance. PD is the second most prevalent neurodegenerative disease among various diseases across the world. According to the World Health Organization, the prevalence of PD has doubled in the past 25 years, and 8.5 million people globally suffer from this disease.<sup>2,3</sup> The etiology of PD is still obscure; however, the main pathophysiology is the presence of  $\alpha$ -Synuclein ( $\alpha$ -Syn) aggregates in Lewy bodies.<sup>4</sup> Moreover, the mutations in the SNCA gene (A30P, E46K, A53T, A53E, H50Q, G51D, and A53V) are critically involved in the familial form of PD.<sup>5</sup> Therefore, it was hypothesized that  $\alpha$ -Syn plays a critical role in the pathophysiology of PD and other synucleopathies.

$\alpha$ -Syn is an intrinsically disordered protein (IDP) comprising of 140 amino acids, mainly present in the brain.<sup>6</sup>  $\alpha$ -Syn consists of three regions: the N-terminal region (1–60 amino acids) containing amphipathic amino acids which help the protein to bind with the membrane, the nonamyloid component (NAC

domain 61–95 amino acids) consisting of hydrophobic amino acids responsible for protein aggregation, and the C-terminal region (96–140 amino acids) containing polar residues which mediate the protein interaction<sup>7</sup> as shown in Figure 1A. In PD,

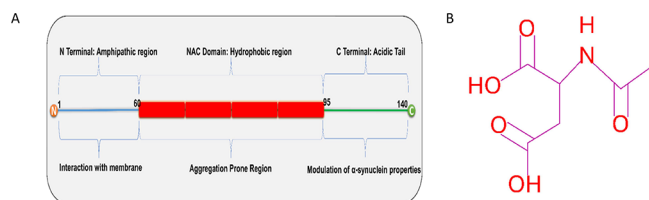


**Figure 1.** (A) Schematic representation of  $\alpha$ -Syn protein depicting the three domains with their function. (B) 2D structure of *N*-acetyl aspartate.

**Received:** January 18, 2024

**Revised:** February 9, 2024

**Accepted:** February 19, 2024

**Published:** February 29, 2024



the neurons containing  $\alpha$ -Syn aggregates in Lewy bodies cause inflammation and neuron degeneration and produce complications such as movement disorders, digestion problems, postural instability, and sleep.<sup>8</sup> The presence of  $\alpha$ -Syn Lewy bodies in the neuron is not only the hallmark of PD but also related to various neurodegenerative disorders, called synucleinopathies.<sup>9</sup> The common manifestation among these diseases is the presence of Lewy bodies of  $\alpha$ -Syn in the affected neurons.

The inhibition of  $\alpha$ -Syn aggregation is considered a promising therapeutic strategy for PD and several other synucleinopathies disorders that are leading causes of dementia worldwide. Protein aggregates can be identified prior to the onset of clinical symptoms in neurodegenerative conditions, making protein aggregation/fibrillation an ideal focus for the development of therapeutic interventions and investigation approaches.<sup>10</sup> Several approaches, such as peptides, small molecules such as tannic acid, curcumin, ellagic acid, resveratrol, and osmolytes like trehalose, and sorbitol, have been used to inhibit  $\alpha$ -Syn aggregation and stabilize the protein in its monomeric form.<sup>11–14</sup> There is presently no preventive treatment in the market, even though several compounds have been identified in the literature for stabilizing the normal conformation of  $\alpha$ -Syn, preventing its aggregation, or dissolving aggregated  $\alpha$ -Syn. In line with this, we need to identify the modulator and/or inhibitor for the therapeutic management of PD.

The role of osmolytes in enhancing the stability of globular proteins is well established, particularly in cells experiencing stress.<sup>15–17</sup> However, the impact of osmolytes on the stability, structure, and aggregation of IDPs remains uncertain. Numerous investigations have been conducted on osmolytes, including trimethylamine *N*-oxide, polysaccharides, and sugars like glucose.<sup>18</sup> The results of these studies revealed the detrimental consequences of preferential exclusion; the strong structural stabilization exerted by these osmolytes induces the formation of more compact ensembles in IDPs. Consequently, this compactness facilitates the aggregation and fibrillation of IDPs.<sup>19–22</sup> On the other hand, it has been also reported that osmolytes also maintain the IDPs in their native form.<sup>23</sup> Additionally, they hinder the production of fibrils by facilitating the assembly of oligomers or the formation of amorphous aggregates.<sup>14</sup> The common mechanism by which osmolytes show paradoxical behaviors on IDPs has not been elucidated yet. However, the controlling parameters for the osmolyte effect on IDPs have been reported, which are chain length, osmolyte viscosity, protein–polymer interactions, and particular amino acid side chain interactions.<sup>15,24,25</sup> The investigations of osmolytes also encompassed an examination of their potential protective influence on the aggregation of  $\alpha$ -Syn. Various polyols, including ethylene glycol, trehalose, erythritol, and glycerol, have been used to see the effect on the aggregation of  $\alpha$ -Syn, and the results demonstrated that an increased concentration of these polyols effectively hampers the aggregation of  $\alpha$ -Syn, whereas a decreased concentration substantially promotes the aggregation process.<sup>13,14</sup> The polyol osmolyte effects have been studied on  $\alpha$ -Syn aggregation; however, the effect of amino acid osmolytes has not been investigated on the protein yet.

*N*-Acetyl aspartate (NAA) is a prominent cerebral amino acid osmolyte that exhibits a substantial presence of up to 10 mM within the neurons.<sup>26</sup> However, the underlying rationale for the extensive synthesis of this acetylated amino acid by neurons is yet to be fully elucidated. Initial investigations suggested that NAA plays a role in the production of lipids in the brain, particularly during the process of postnatal myelination.<sup>27</sup>

Several studies have established a correlation between NAA and transportation of carbon as well as the metabolism of energy in the mitochondria within the neurons.<sup>28</sup> NAA has been investigated as an osmoprotectant front for protein stability.<sup>29</sup> Moreover, NAA has shown an antiglycation effect on irisin protein.<sup>30</sup> To date, the NAA roles have not been studied for the modulation of protein aggregation. Hence, our study aimed to examine the impact of NAA on the aggregation of  $\alpha$ -Syn. In this study, we used various aggregation assays, such as ThT, RLS, ANS, turbidity, and microscopical observation, to monitor the impact of varying concentrations of NAA on  $\alpha$ -Syn aggregation. We found an interesting observation that NAA shows a paradoxical effect on  $\alpha$ -Syn aggregation; that is, lower concentrations of NAA were inhibiting the  $\alpha$ -Syn aggregation, whereas higher concentrations of NAA were accelerating the  $\alpha$ -Syn aggregation. Further, we performed interaction studies such as fluorescence binding and molecular docking studies to check the binding affinity of NAA toward  $\alpha$ -Syn. We found that NAA has moderate binding affinity for  $\alpha$ -Syn. The findings suggest that NAA plays a significant role as an osmoprotectant in preventing the  $\alpha$ -Syn fibrillation at lower concentrations, and therefore NAA could potentially be involved in the therapeutic treatment of PD.

## 2. MATERIALS

Streptomycin sulfate, IPTG, and NAA were purchased from Sigma Chemical (St. Louis, MO, USA). The expression construct of  $\alpha$ -synuclein (pET21a- $\alpha$ -Syn) was procured from Addgene (plasmid # 51486). BL-21-DE3 and DHS $\alpha$  cells were procured from Invitrogen (USA). For purification, glacial acetic acid, ammonium acetate, and ammonium sulfate were procured from Merk. Tris, Luria Bertini media, and ampicillin were purchased from MP Biomedicals, LLC (France).

**2.1. Methods.** **2.1.1. Protein Expression and Purification.** The clone of pET21a- $\alpha$ -Syn (Addgene plasmid ID- 51486) was gifted by the Michael J. Fox Foundation. The expression and purification of wild-type  $\alpha$ -Syn were carried out using previously reported methods with slight modifications.<sup>31</sup> Briefly, the pET21a- $\alpha$ -Syn expression construct was transformed in BL-21 (DE3) competent cells and expressed under 1 mM IPTG conditions at 37 °C. IPTG-induced cells were then centrifuged at 6000g for 15 min, and the pellets were resuspended in the lysis buffer (50 mM tris pH 7.5, 150 mM NaCl, 10 mM EDTA, and 1 mM PMSF). The lysed pellets were sonicated at 50% amplitude with 50 pulses/min for 15 min at 4 °C. The samples were then centrifuged at 10,000g for 30 min, and the supernatant was heated at 95 °C for 20 min. The supernatant after centrifugation was treated with 10% streptomycin sulfate and glacial acetic acid to precipitate the DNA. The samples were further centrifuged at 12,000g, and the supernatant was treated with saturated ammonium sulfate and incubated at 4 °C for 12 h. The protein precipitated by saturated ammonium sulfate was washed three times with chilled ethanol to remove the ammonium sulfate. The purified protein was snap-chilled with liquid nitrogen and then underwent lyophilization. The lyophilized protein powder was resuspended in 10 mM tris pH 7.5 and 150 mM NaCl. The protein solution was further purified by a Gel-filtration AKTA pure system using a superdex 200 pg column. The purity of  $\alpha$ -Syn was checked by 15% SDS PAGE.

**2.1.2. Preparation of Low-Molecular-Weight  $\alpha$ -Syn.** Low-molecular-weight (LMW)  $\alpha$ -Syn was prepared by passing the purified protein through a gel-filtration chromatography to a 100 kDa Centricon. The flow through of the passed solution from

the Centricon possesses LMW  $\alpha$ -Syn. The concentration of LMW  $\alpha$ -Syn was then calculated using molar extinction coefficients  $5960 \text{ M}^{-1} \text{ cm}^{-1}$  at  $280 \text{ nm}$ .<sup>32</sup> The obtained LMW  $\alpha$ -Syn was used for the experimental studies.

**2.1.3. Sample Preparation for Aggregation Study.**  $\alpha$ -Syn ( $70 \mu\text{M}$ ) was incubated in the absence and presence of 2, 5, 15, and 20 mM concentrations of NAA in 10 mM Tris pH 7.5, 150 mM NaCl at  $37^\circ\text{C}$  with 220 rpm in the incubator shaker for 96 h. In the samples, sodium azide (0.02%) was added to avoid microbial contamination. The aliquots were withdrawn at specific time intervals from the incubated samples and proceeded for further experiments.

**2.1.4. Time-Dependent ThT Aggregation Kinetic Study.** ThT, also known as thioflavin T, is a fluorescent dye commonly employed to monitor protein aggregation, owing to its ability to selectively bind to amyloid fibrils, which are protein aggregates commonly associated with neurodegenerative diseases.<sup>33</sup> ThT was dissolved in water and filtered through a  $0.22 \mu\text{M}$  syringe filter, and its concentration was determined by taking the absorbance at  $412 \text{ nm}$  using  $\epsilon_{412} = 24,420 \text{ M}^{-1} \text{ cm}$ .<sup>34</sup> The aliquots withdrawn at specific time intervals from the incubated samples were diluted to  $15 \mu\text{M}$  and incubated with  $20 \mu\text{M}$  ThT for 15 min in the dark.<sup>35</sup>

Three independent ThT fluorescence measurements of the sample were taken by a Jasco FP-8200 fluorescence spectrometer with an excitation wavelength of  $440 \text{ nm}$  and the emission wavelength in the range of  $450\text{--}600 \text{ nm}$ .<sup>36</sup> All of the measurements were taken in triplicate with an error of less than 4%. Aggregation parameters ( $T_{\text{agg}}$ ,  $T_{\text{lag}}$ , and  $b$ ) were analyzed through eq 1 using a nonlinear regression method using Sigma plot 10.0.

$$A = A_0 + \frac{A_{\text{max}}}{1 + e^{-(T - T_{\text{agg}})/b}} \quad (1)$$

where  $A$  is the fluorescence intensity (F.I.) at any time  $T$ ,  $A_{\text{max}}$  corresponds to the F.I. observed at the final plateau line,  $b$  denotes a constant value that remains unaffected by time at a given wavelength,  $A_0$  represents the F.I. of the initial baseline and osmolyte concentration, and  $T_{\text{agg}}$  refers to the time of 50% of maximum F.I.  $T_{\text{lag}}$  was calculated by putting the value of  $T_{\text{agg}}$  in  $(T_{\text{agg}} - 2b)$ .<sup>10</sup>

**2.1.5. ANS Assay.** 8-Anilino-1-naphthalene sulfonic acid (ANS) dye binds to the exposed hydrophobic patches of protein and is employed to monitor the intermediate stages during aggregation.<sup>37</sup> The preparation of ANS stock was performed in phosphate buffer pH 7.5, and its concentration was calculated by taking the absorption maximum at  $350 \text{ nm}$  using molar extinction coefficient  $\epsilon_{350} = 5000 \text{ M}^{-1} \text{ cm}$ . The aliquots withdrawn at specific time intervals were diluted to  $15 \mu\text{M}$ . ANS was added to the aliquoted protein samples in the ratio of 1:20.<sup>38</sup> The ANS fluorescence measurements were taken by a Jasco FP-8200 spectrofluorometer using an excitation wavelength of  $380 \text{ nm}$ , and the emission range was recorded between  $400$  and  $650$ .<sup>39</sup> All measurements were carried out in triplicates.

**2.1.6. Turbidity Measurement.** The turbidity in the samples was measured at a wavelength of  $350 \text{ nm}$  using a cuvette with a path length of  $10 \text{ mm}$  employing a UV–visible spectrophotometer manufactured by Shimadzu.<sup>40</sup> The samples were collected at specified times and subsequently diluted to a concentration of  $15 \mu\text{M}$ . Afterward, the absorbance measurement for the samples was carried out at a wavelength of  $350 \text{ nm}$ .

**2.1.7. Rayleigh Light Scattering.** Rayleigh light scattering (RLS) was measured on a Jasco FP-8200 fluorescence spectrophotometer. The aliquots drawn at specific time intervals from the incubated samples at  $37^\circ\text{C}$  were diluted to  $15 \mu\text{M}$ . The measurement of RLS was carried out using excitation wavelengths of  $350 \text{ nm}$  and an emission range of  $300\text{--}400 \text{ nm}$  with a slit width of  $5 \text{ nm}$ .<sup>39</sup>

**2.1.8. Circular Dichroism Spectroscopy.** Circular dichroism (CD) spectroscopy was employed to observe the secondary structural alteration of the protein. The measurement of secondary structural changes in the far-UV CD range ( $190\text{--}250 \text{ nm}$ ) was conducted on a Jasco spectropolarimeter (model J-1500). The aliquots were drawn at 0 and 96 h from the incubated samples at  $37^\circ\text{C}$  and were diluted to  $15 \mu\text{M}$ . The diluted  $15 \mu\text{M}$   $\alpha$ -Syn was filled in a cuvette of path length  $1 \text{ mm}$  and read at the scanning rate of  $100 \text{ nm/min}$ . The baseline was performed with 10 mM Tris and 150 mM NaCl pH 7.5.

**2.1.9. Confocal Microscopy.** Confocal microscopy was employed to visualize the protein aggregates. The samples were aliquoted at 0 and 96 h and stained with the ThT dye and visualized using confocal microscopy (Nikon Eclipse Ti, Japan). The samples were aliquoted and, thereafter, combined with the probe in a 1:1 molar ratio. The resulting mixture was then incubated in the dark for a duration of 15 min. Subsequently, extensive washing was performed, and the samples were excited by using a fixed  $405 \text{ nm}$  laser line and observed the fluorescence light in the range of  $420\text{--}520 \text{ nm}$ . The visualization was carried out by confocal microscopy with a  $63\times$  oil immersion objective.

**2.1.10. Interaction Studies.** **2.1.10.1. Fluorescence Quenching Studies.** To investigate the NAA and  $\alpha$ -Syn interaction, a fluorescence-binding study was conducted following a previously established procedure.<sup>41</sup> For conducting fluorescence quenching investigations, a concentration of  $50 \mu\text{M}$   $\alpha$ -Syn was utilized, and spectrum measurements were performed using a Jasco spectrofluorometer manufactured by Jasco in Japan. The excitation was performed using a wavelength of  $274 \text{ nm}$ , while the measurement of emission spectra was taken in the range of  $300\text{--}400 \text{ nm}$ . The slit widths of excitation and emission were set at  $10 \text{ nm}$ . The estimation of various binding parameters was conducted by mathematically analyzing the fluorescence quenching of  $\alpha$ -Syn with increasing concentrations of NAA. This analysis utilized the Stern–Volmer equation (eq 2)<sup>42</sup> and the double-logarithmic equation (eq 3).<sup>43</sup>

$$\frac{F_0}{F} = 1 + K_{\text{sv}}[C] \quad (2)$$

The variables  $F_0$  and  $F$  represent the fluorescence intensity of  $\alpha$ -Syn and  $\alpha$ -Syn with NAA, respectively.  $[C]$  depicts the different concentrations of NAA. Stern–Volmer constant is denoted by  $K_{\text{sv}}$ .

$$\log \frac{F_0 - F}{F} = \log K + n \log [C] \quad (3)$$

The symbol “ $K$ ” represents the binding constant of the complex formed between  $\alpha$ -Syn and NAA. The concentration of NAA is denoted by “ $[C]$ ,” while the variable “ $n$ ” represents the number of binding sites.

**2.1.10.2. Molecular Docking.** The binding affinity of NAA was evaluated by molecular docking simulations conducted on the  $\alpha$ -Syn protein. The nuclear magnetic resonance structure of  $\alpha$ -Syn (PDBID: 1xq8) was employed as an initial reference for the docking investigations. The ligands’ three-dimensional structures were acquired from the PubChem database in SDF

format utilizing PubChem IDs. The process of ligand docking onto the protein was conducted via AutoDock Vina software on the UCSF Chimera platform. The ligand that was protonated and subjected to geometry optimization was utilized for the docking investigations. The protein and ligand were produced for the docking studies using the Dock Prep module. Additional charges were imposed by Gasteiger. The docking procedure was conducted to anticipate 10 binding possibilities while ensuring that the highest energy difference between them did not exceed 3 kcal/mol. The level of comprehensiveness in the search was established to be a maximum of 8. The docked states generated by Vina were further subjected to analysis in order to identify the most likely area of ligand binding as well as the specific residues and types of interactions involved. The analysis of docking results was carried out with Discovery Studio Visualizer and PyMOL tools.

### 3. RESULTS

**3.1. NAA Modulates  $\alpha$ -Syn Fibrillation.** **3.1.1. ThT Fluorescence Assay.** To examine the effect of NAA on the aggregation of  $\alpha$ -Syn, we performed a time-dependent ThT binding assay. ThT is a benzothiazole dye that exhibits a specific binding affinity toward amyloid fibrillar structures.<sup>44</sup> This characteristic renders it suitable for use as a probe in the identification and measurement of amyloid fibrils. Enhanced fluorescence intensity is observed because of the interaction between ThT and the cross-beta structure of the fibrils. Consequently, the ThT assay was employed to monitor the aggregation kinetics of  $\alpha$ -Syn without and with different NAA concentrations at pH 7.5 and 25 °C. Figure 2 shows the

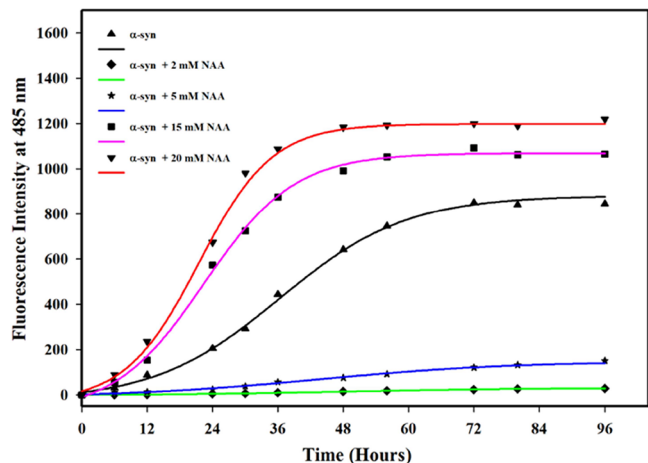


**Figure 2.** Aggregation kinetics of  $\alpha$ -Syn in the presence of different concentrations of NAA.

fibrillation profile of  $\alpha$ -Syn without and with varying NAA concentrations for a duration of 96 h. The figure indicates that the ThT fluorescence of  $\alpha$ -Syn alone increases with time and shows a typical sigmoidal curve, which suggests the nucleation-dependent aggregation pathway of  $\alpha$ -Syn as per a previous report. The nucleation-dependent pathway of  $\alpha$ -Syn aggregation starts with the lag phase that was marked by the formation of the nucleus, followed by the exponential/log phase that related to the fibril's elongation, and eventually reaches a stationary phase. A significant reduction in ThT fluorescence was observed at various time intervals when subjected to NAA concentrations of 2 and 5 mM. Nevertheless, a noteworthy enhancement in the

ThT fluorescence intensity was observed with 15 and 20 mM NAA with increasing time. This observation suggests the paradoxical nature of NAA in  $\alpha$ -Syn aggregation. We have calculated the aggregation kinetic parameters such as  $T_{lag}$  and  $T_{agg}$  by fitting the aggregation kinetic curve of  $\alpha$ -Syn alone and with different concentrations of NAA in eq 1 as shown in Table 1. It was observed that 2 and 5 mM NAA increase the lag time, thereby preventing the  $\alpha$ -Syn aggregation to the maximum level.

**Table 1. Various Aggregation Parameters Obtained from the Aggregation Kinetics of  $\alpha$ -Syn Alone and with Varying Concentrations of NAA**

concentration (mM)	$b$	$T_{agg}$	$T_{lag} (T_{agg} - 2b)$ (h)
0	6.48	35.79	22.83
2.0	9.01	48.43	30.43
5.0	9.76	47.84	28.32
15.0	5.20	23.09	12.69
20.0	4.33	21.08	12.43

**3.1.2. Turbidity Assay.** To confirm the paradoxical nature of NAA on  $\alpha$ -Syn aggregation, a turbidity assay was employed to corroborate the ThT result. The measurement of turbidity using absorbance is a widely employed and inexpensive technique for monitoring protein aggregation. Turbidity describes the opaqueness of the solution, resulting from discrete particles. Most proteins exhibit minimal absorbance at a wavelength of 350 nm. Consequently, a significant absorbance at this wavelength serves as an indicator of protein aggregates, which arise from the scattering of light by large aggregated particles. In this experiment, the samples were subjected to incubation for a duration of 72 h under the aggregation conditions. Turbidity measurements were subsequently recorded at a wavelength of 350 nm at definite time intervals. Figure 3 shows the extent of

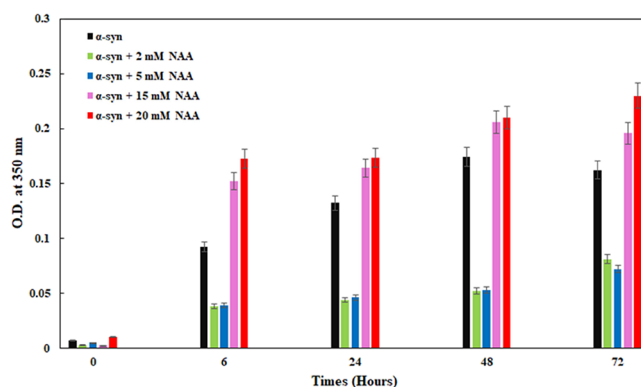


**Figure 3.** Time-dependent turbidity measurement of  $\alpha$ -Syn in the presence of various concentrations of NAA. Standard errors in the mean from at least three measurements are shown by error bars.

absorbance caused by  $\alpha$ -Syn alone and  $\alpha$ -Syn with varying concentrations of NAA at definite time intervals. The high turbidity was observed for  $\alpha$ -Syn alone as a function of time, suggesting the fibril formation that makes the solution more turbid. In the presence of 2 and 5 mM NAA, the absorbance at 350 nm decreases with time. However, with a high concentration of NAA, the solution became more turbid with time, which may be due to  $\alpha$ -Syn aggregation.

**3.1.3. RLS Measurement.** RLS is more sensitive than turbidity assay in terms of understanding the dimensions of

protein aggregates. Rayleigh scattering refers to the phenomenon of electromagnetic radiation being dispersed by particles present in a protein solution.<sup>45</sup> This scattering may be quantified using a spectrofluorometer wherein the excitation and emission wavelengths of the radiation coincide. The utilization of RLS as a highly accurate method by researchers for assessing the degree of aggregation in protein solutions involves employing an excitation wavelength of 350 nm and an emission range from 300 to 400 nm. Figure 4 shows the extent of light scattering

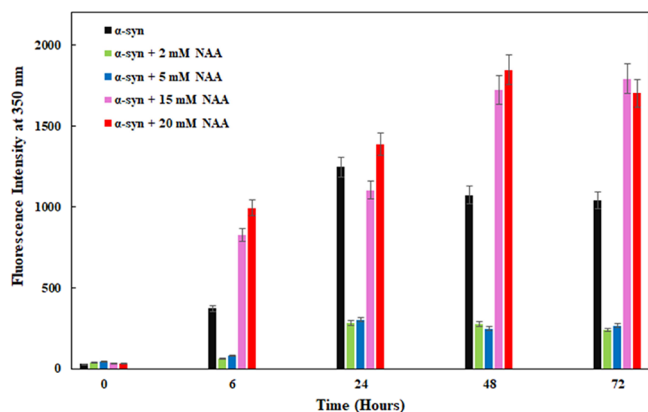


**Figure 4.** Time-dependent RLS measurement of  $\alpha$ -Syn in the presence of various concentrations of NAA. Standard errors in the mean from at least three measurements are shown by error bars.

caused by  $\alpha$ -Syn alone and with different concentrations of NAA at definite time intervals. The light scattered by  $\alpha$ -Syn alone increased with time indicating the formation of protein aggregates. In the presence of 2 and 5 mM NAA, there was no such light scattering observed which may be due to less aggregated particles of  $\alpha$ -Syn. However, the extent of light scattering was more in the case of high concentration of NAA which may be due to the presence of large aggregates. These results of turbidity and RLS corroborate the ThT observations and suggest the paradoxical nature of NAA toward the  $\alpha$ -Syn aggregation.

**3.1.4. ANS Measurement.** The process of protein aggregation and fibrillation is accelerated by the presence of hydrophobic patches. The presentation of hydrophobic regions on proteins expedites the binding of monomer units, ultimately resulting in the creation of protein clumps or fibrils.<sup>46</sup> ANS is a fluorescent dye commonly employed to interact with hydrophobic regions found on protein surfaces. The ANS assay is commonly employed to assess the protein surface hydrophobicity. For ANS measurements, the wavelength used for excitation is 380 nm, and the emission wavelength is recorded in the range of 400–600 nm. ANS dye was mixed with the protein samples with and without NAA in a ratio of 1:20, and measurements were taken after incubating the samples for 30 min in the dark. Figure 5 shows the ANS fluorescence caused by  $\alpha$ -Syn alone and with different concentrations of NAA at definite time intervals. At 0 h, there was negligible ANS fluorescence observed for  $\alpha$ -Syn alone, and very minimal hydrophobic patches were present in the protein with varying concentrations of NAA. The maximum ANS fluorescence was observed for  $\alpha$ -Syn alone and with 15 and 20 mM NAA at 48 h. These observations suggested the presence of exposed hydrophobic patches on the protein surface, which may provide the prerequisite condition for  $\alpha$ -Syn aggregation. However, there was very low ANS fluorescence observed for the

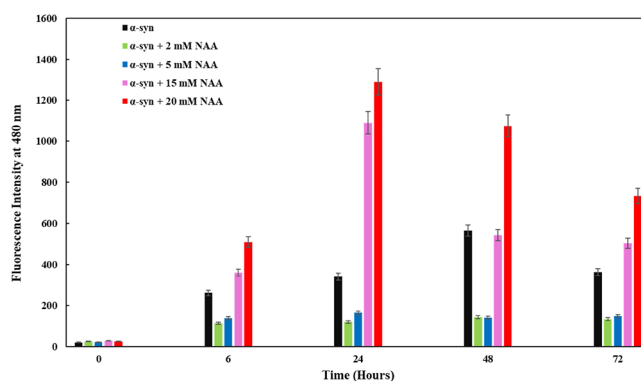


**Figure 5.** Time-dependent ANS measurement of  $\alpha$ -Syn in the presence of various concentrations of NAA. Standard errors in the mean from at least three measurements are shown by error bars.

lower concentrations of NAA, i.e., 2 and 5 mM NAA, suggesting that lower concentrations of NAA maintain the  $\alpha$ -Syn in the monomeric form. Further, the ANS fluorescence was decreased for  $\alpha$ -Syn alone and higher concentrations of NAA at 72 h as compared to 48 h, suggesting that most of the exposed hydrophobic patches could be utilized for the fibril formation and not available for binding with the ANS dye. Thus, the ANS fluorescence result suggests that NAA modulates the hydrophobic interactions of  $\alpha$ -Syn that are critical for protein aggregation. A relatively enhanced ANS intensity was observed in high concentrations of NAA as compared to lower concentrations of NAA and  $\alpha$ -Syn alone, suggesting a higher change in the surface hydrophobicity of the protein.

**3.2. CD Spectroscopy.**  $\alpha$ -Syn is primarily found in an extended conformation and exists as an IDP under physiological conditions. Nevertheless, it does give rise to transient oligomeric entities that consist of  $\alpha$ -helices and, afterward, undergo a transformation into cross  $\beta$ -sheet fibrils. Thus, CD spectroscopy was utilized to observe the changes in the secondary structure of  $\alpha$ -Syn upon exposure to different concentrations of NAA with time. Figure 6 illustrates the CD spectra in the far-UV region of  $\alpha$ -Syn alone as well as with different concentrations of NAA at 0 and 96 h.  $\alpha$ -Syn alone and with 2 and 20 mM NAA at 0 h show a large negative peak at  $\sim$ 200 nm, which suggests the presence of random coil conformation. At 96 h, a large negative peak at 218

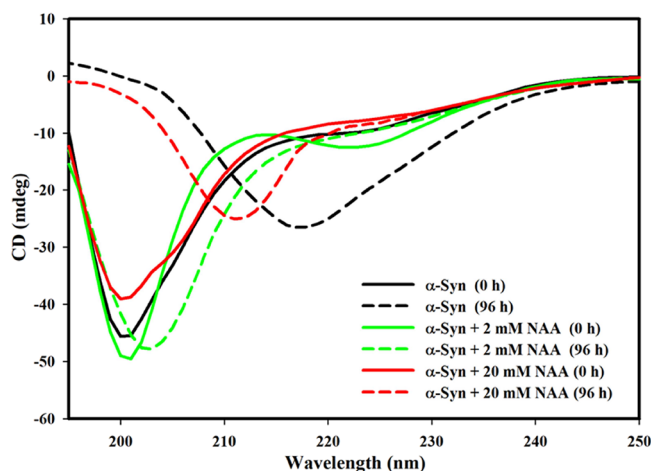


**Figure 6.** Time-dependent far-UV CD measurement of  $\alpha$ -Syn in the presence of various concentrations of NAA.

nm in the  $\alpha$ -Syn alone sample was observed, which suggests that  $\alpha$ -Syn started forming  $\beta$ -sheet-rich amyloid fibrils. However,  $\alpha$ -Syn in the presence of 2 mM NAA shows a negative peak at  $\sim$ 200 nm, which suggests that 2 mM NAA retains the structure of  $\alpha$ -Syn in the random coil structure, whereas  $\alpha$ -Syn with 20 mM NAA shows a negative peak around 210 nm, suggesting that 20 mM NAA did not maintain the  $\alpha$ -Syn in its native random coil structure and initiates the formation of  $\beta$ -sheet-rich fibrils of  $\alpha$ -Syn. The far-UV CD results further corroborate the previous results of ThT, turbidity, and RLS, suggesting the paradoxical behavior of NAA on  $\alpha$ -Syn aggregation.

**3.3. Confocal Microscopy.** To corroborate the ThT, Turbidity, and CD results of NAA showing the paradoxical behaviors on  $\alpha$ -Syn aggregation, we employed confocal laser scanning microscopy to investigate the NAA behaviors on the morphology of the  $\alpha$ -Syn aggregates. Here, ThT as a fluorescent dye was used to stain the protein samples as it gives fluorescence emission on binding with protein aggregates. Figure 7A depicts

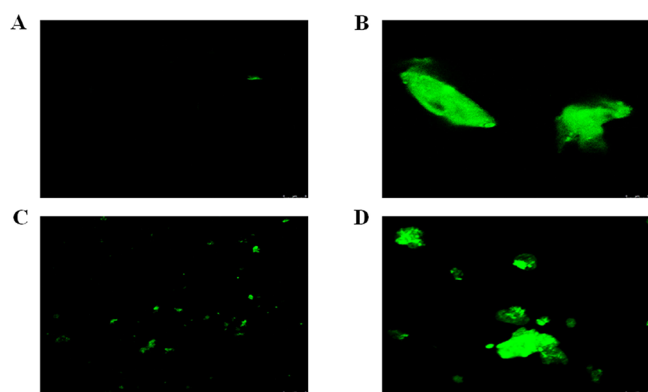


**Figure 7.** Confocal microscopic images of (A)  $\alpha$ -Syn at 0 h and (B) aggregated  $\alpha$ -Syn at 96 h. (C)  $\alpha$ -Syn incubated with 2 mM NAA after 96 h. (D)  $\alpha$ -Syn incubated with 20 mM NAA after 96 h.

that the native  $\alpha$ -Syn at 0 h lacks fibril structure and shows no fluorescence under confocal microscopy as ThT specifically binds to the amyloid. The incubated  $\alpha$ -Syn after 96 h in aggregation condition shows a fibril-type structure and emits strong fluorescence as shown in Figure 7B, which suggests that  $\alpha$ -Syn formed a fibril. Figure 7C shows that  $\alpha$ -Syn incubated with 2 mM NAA after 96 h shows very little aggregated structure, which suggests that 2 mM NAA inhibits the fibrillation of  $\alpha$ -Syn. However, a large and greater number of aggregated structures were observed in the case of  $\alpha$ -Syn incubated with 20 mM NAA after 96 h as shown in Figure 7D, suggesting that 20 mM NAA aggravates the  $\alpha$ -Syn aggregation. These observations from the microscopy further support the paradoxical effect of NAA on the aggregation of  $\alpha$ -Syn.

**3.4. Interaction Studies of  $\alpha$ -Syn with NAA.** **3.4.1. Fluorescence Quenching Studies.** The binding studies of proteins with ligands are critical to understanding the mechanisms of regulation of biologically crucial processes, such as immune response, cell regulation, and signal transduction. The comprehension of the protein–ligand binding mechanism holds significant importance due to its fundamental role in the identification, design, and exploration of novel therapeutic agents.<sup>47–49</sup> Various assays conducted in this study suggest that NAA acts paradoxically on  $\alpha$ -Syn aggregation. It is important to know whether NAA binds with the  $\alpha$ -Syn monomer or not. In line with this, we carried out the fluorescence quenching study to

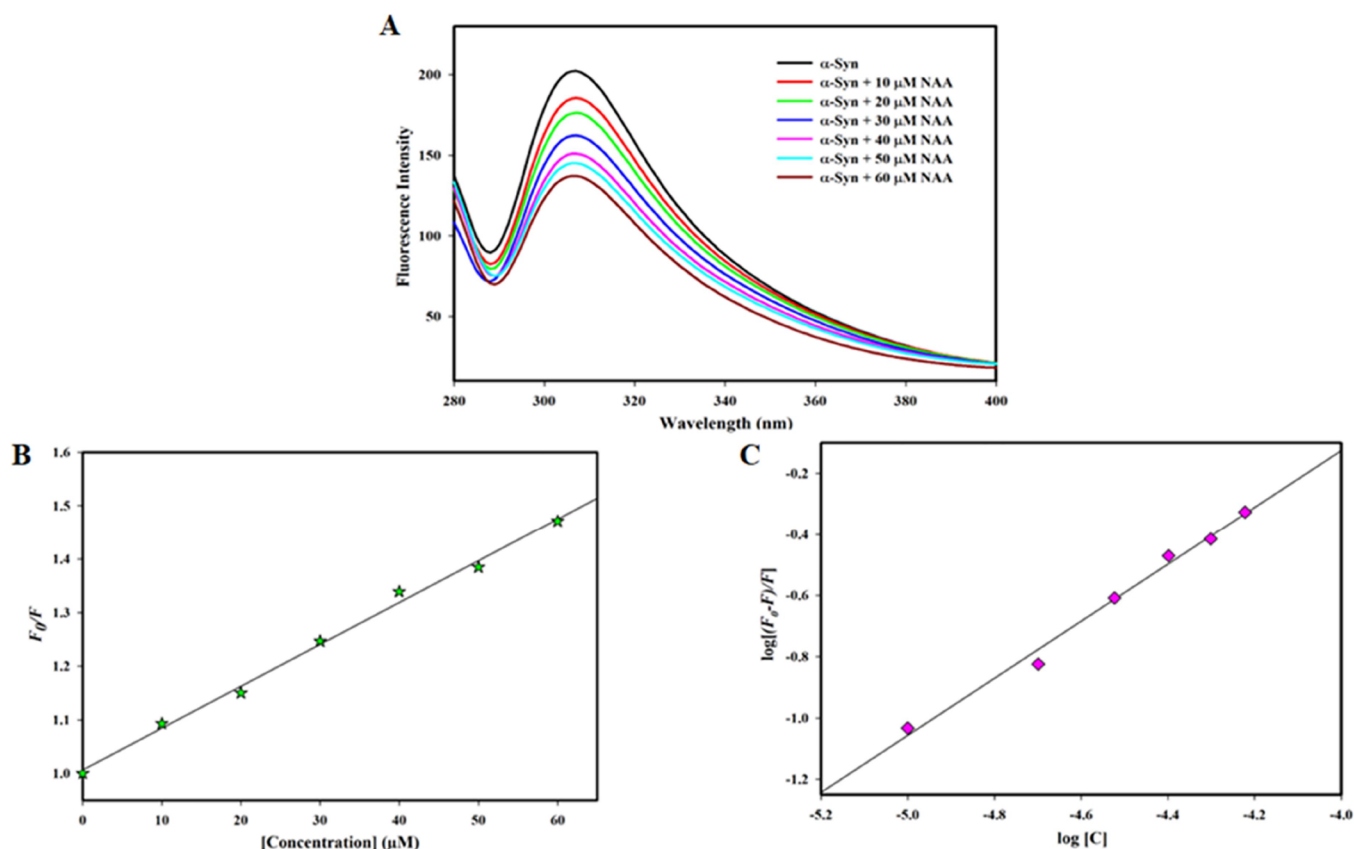
understand the binding of NAA to  $\alpha$ -Syn. Fluorescence spectroscopy is commonly utilized in scientific research to examine the interaction between proteins and ligands, providing multiple parameters that aid in the comprehension of the degree of the interaction. The phenomenon of a decreased fluorescence intensity of protein with an increasing concentration of the ligand is known as fluorescence quenching. The structural composition of  $\alpha$ -Syn has an unequal distribution of four tyrosine residues, resulting in the intrinsic fluorescence of  $\alpha$ -Syn relying on these specific tyrosine residues.  $\alpha$ -Syn contains four tyrosine residues: Tyr 39 is present at the N-terminal region, whereas others Tyr 125, Tyr 133, and Tyr 136, are present in the C-terminal region. The measurement of tyrosine quenching was conducted using an excitation wavelength of 275 nm, and the emission was recorded within the wavelength range of 290–400 nm. Figure 8A depicts the Tyr quenching spectra of  $\alpha$ -Syn (50  $\mu$ M) with increasing concentrations of NAA (0–60  $\mu$ M). The observed decrease in the tyrosine fluorescence of  $\alpha$ -Syn as the concentration of the ligand increases suggests that there is an interaction between  $\alpha$ -Syn and NAA.

Figure 8 B,C depict the modified Stern–Volmer plots of  $\alpha$ -Syn, illustrating a direct correlation between the fluorescence quenching intensity and NAA. The binding constant  $0.45 \times 10^4 \text{ M}^{-1}$  was observed for NAA with monomeric  $\alpha$ -Syn, which indicates a moderate binding affinity with  $\alpha$ -Syn.

**3.4.2. Molecular Docking.** Molecular docking techniques play a pivotal role in the field of computational chemistry and are frequently employed to elucidate the mechanisms behind target–drug interactions in modern drug discovery attempts.<sup>50</sup> There are several molecular docking technologies, such as AutoDock Vina, that can be utilized to assess the binding affinity between ligands and proteins. In this investigation, the AutoDock Vina program was employed to identify the optimal binding pose for investigating the protein–ligand interactions. The specific binding sites of  $\alpha$ -Syn were not previously identified; hence, a blind docking approach was employed to determine the potential binding sites. Among the nine conformations generated via docking, the best-docked conformation is shown in Figure 9. The molecular docking analysis reveals that NAA exhibits a moderate binding affinity of  $-4.2 \text{ kcal mol}^{-1}$  toward  $\alpha$ -Syn. Figure 9A shows the  $\alpha$ -Syn monomer as a blue ribbon docked with NAA as depicted in red with a ball and stick model. Figure 9B shows that NAA interacts with the C-terminus of  $\alpha$ -Syn; it mainly interacts with the Met127, Glu126, Glu130, and Pro128 residues of  $\alpha$ -Syn through a hydrogen bond. The interaction of NAA with  $\alpha$ -Syn was also stabilized with van der Waals interaction by Tyr125 and Ser129 residues. Figure 9C,D depicts that NAA is present in the deep cavity of the  $\alpha$ -Syn binding pocket. Therefore, all of these *in silico* results corroborate the fluorescence quenching studies of  $\alpha$ -Syn with NAA, suggesting that NAA forms a complex with the  $\alpha$ -Syn monomer with a moderate binding affinity.

## 4. DISCUSSION

PD is a neurodegenerative disorder that impacts both peripheral and central nervous systems of the human brain. It counts as the second most prevalent neurological disease globally.<sup>51</sup> The development of Lewy bodies and Lewy neurites, which are recognized as the characteristic features of PD, is attributed to the existence of insoluble intraneuronal inclusions of the  $\alpha$ -Syn protein. Numerous small-molecule inhibitors have been reported for the inhibition of  $\alpha$ -Syn aggregation to combat PD. Osmolytes refer to small organic molecules that are released



**Figure 8.** (A) Fluorescence spectra of  $\alpha$ -Syn in the presence of varying concentrations of NAA (0–60  $\mu$ M). (B) Stern–Volmer plot of  $\alpha$ -Syn with varying concentrations of NAA (0–60  $\mu$ M). (C) Double log relation of  $\alpha$ -Syn–NAA.

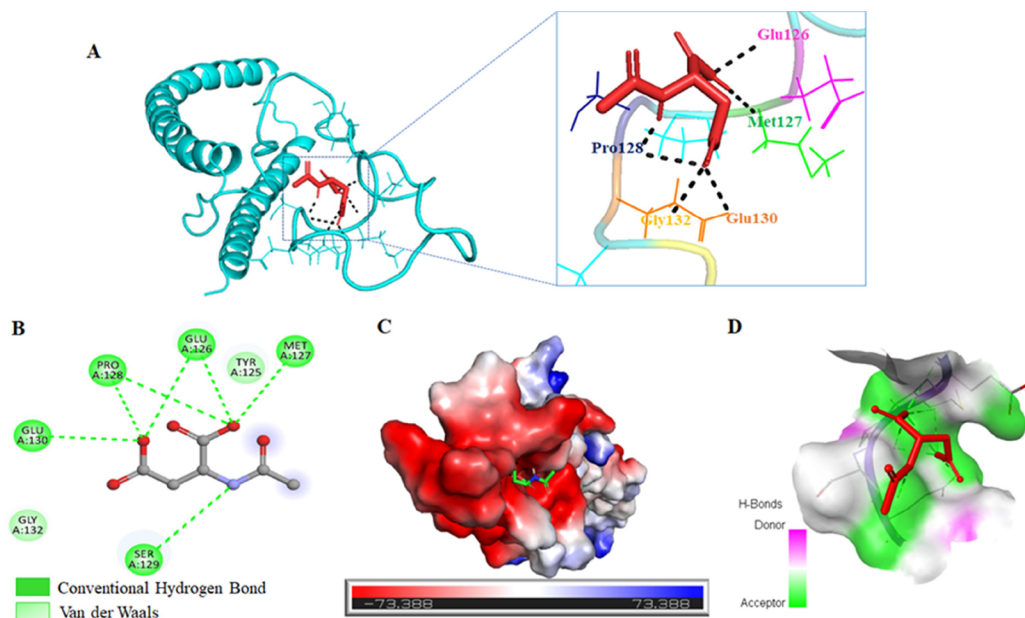


**Figure 9.** Structural representation of the interaction of  $\alpha$ -Syn with NAA. (A) Docked complex of  $\alpha$ -Syn with NAA showing hydrogen bonded residues of  $\alpha$ -Syn. (B) 2D interaction of NAA with binding pocket residues of  $\alpha$ -Syn. (C) Charged surface view of  $\alpha$ -Syn complexed with NAA. (D) Surface image of the NAA-occupied  $\alpha$ -Syn binding pocket.

by cells in response to severe stress conditions.<sup>52</sup> Numerous studies have shown that polyols osmolytes have a stabilizing effect on  $\alpha$ -Syn monomers and inhibit the  $\alpha$ -Syn aggregation.<sup>11,14,34</sup> However, the impact of amino acid osmolytes on  $\alpha$ -Syn aggregation has not yet been elucidated yet. NAA is an

amino acid osmolyte that is mainly present in the brain in high concentrations of up to 10 mM.<sup>29</sup> The presence of such a high concentration of NAA in the brain is still a matter of debate.

Herein, we have expressed, purified, and biophysically characterized the  $\alpha$ -Syn protein and investigated the impact of

NAA on  $\alpha$ -Syn aggregation by using various spectroscopic methods as well as confocal microscopy. For aggregation studies, the samples containing  $\alpha$ -Syn without and with different concentrations of NAA were incubated at 37 °C for 96 h while being agitated at a speed of 220 rpm. ThT assay was employed to monitor the aggregation kinetics of  $\alpha$ -Syn alone and with concentrations of NAA at pH 7.5. It was found that the lower concentration of NAA increases the lag time and prevents aggregation to a maximum level. It is suggested that a lower concentration of NAA may bind with the monomers of  $\alpha$ -Syn and prevent its aggregation. However, the higher concentration of NAA decreased the lag time from 22.83 to 12.43 h. The observation indicates that a higher concentration of NAA could increase the surface hydrophobicity of  $\alpha$ -Syn, thereby accelerating its aggregation. These results revealed the paradoxical nature of NAA on  $\alpha$ -Syn aggregation. Further, turbidity and RLS assay were employed to complement the result of ThT. The increase in the turbidity and RLS with time in the presence of a higher concentration of NAA indicates the presence of aggregated particles in the sample, whereas with a lower concentration of NAA, RLS, and turbidity have not been increased with time. The results of RLS and turbidity suggest that NAA acts paradoxically against  $\alpha$ -Syn aggregation and corroborated the ThT observations. Moreover, ANS assay was employed to monitor the presence of exposed hydrophobic patches on  $\alpha$ -Syn with and without NAA. The ANS results suggested that exposed hydrophobic patches on the surface of  $\alpha$ -Syn decreased with lower concentrations of NAA, whereas higher concentrations of NAA increased the hydrophobic patches on the protein. The result of ANS indicates that higher concentrations of NAA destabilized the  $\alpha$ -Syn protein, and thereby hydrophobic patches were more available for binding to ANS and gave strong fluorescence, whereas lower concentrations of NAA stabilized the  $\alpha$ -Syn monomer as hydrophobic patches were not available for binding with ANS. CD spectroscopy was used to observe the secondary structural changes in  $\alpha$ -Syn without and with NAA during aggregation. It was observed that the secondary structural transition was more pronounced in  $\alpha$ -Syn with a high concentration of NAA, suggesting the formation of a beta-sheet amyloid fibril. However, the lower concentration of NAA maintains the native random coil structure of  $\alpha$ -Syn, indicating stabilization of  $\alpha$ -Syn in its monomeric form. For visualization of aggregates, confocal microscopy was used as it gives higher contrast imaging that helps in visualization of aggregates present in small numbers. The observation of confocal microscopy revealed that more aggregated structures were present in higher concentrations of NAA, whereas less aggregated structures were present in lower concentrations of NAA. All of these results suggested that NAA acted paradoxically on  $\alpha$ -Syn fibrillation. These complex observations of NAA on  $\alpha$ -Syn fibrillation could be explained by the solvophobic effect.<sup>20</sup>  $\alpha$ -Syn, as a protein that lacks a defined structure, contains a high proportion of polar amino acids present at the C-terminus region which makes  $\alpha$ -Syn hydrophilic in nature.<sup>8</sup> NAA exhibits hydrophilicity and carries a negative charge, leading to its anticipated contact with the polar side chains of  $\alpha$ -Syn. However, this association is expected to have a lower affinity in comparison with its interactions with nearby water molecules. When the concentration of NAA increases, the interaction between NAA and water would probably become stronger. As a result, there could be a stronger exclusion of NAA from the surface of  $\alpha$ -Syn. Additionally, the hydrophobic patches of nonpolar amino acids in the NAC

domain of  $\alpha$ -Syn are anticipated to experience the repulsive interactions. These interactions could cause unfolded  $\alpha$ -Syn to compact. The compaction of the unfolded monomer of  $\alpha$ -Syn may lead to an increase in the density of hydrophobic side chains in its proximity, thereby increasing intramolecular contacts.<sup>53</sup> These interactions, in turn, encourage intermolecular interactions, ultimately resulting in self-association and oligomerization of  $\alpha$ -Syn. All these observations of aggregation assays suggested that NAA acting paradoxically could be due to the solvophobic effect. To further confirm the hypothesis, we carried out the interaction studies of  $\alpha$ -Syn with NAA by fluorescence quenching methods as well as by molecular docking studies to determine the binding affinity and critical residues involved in the interaction. Fluorescence quenching studies revealed that NAA binds with  $\alpha$ -Syn with moderate binding affinity of  $0.45 \times 10^4 \text{ M}^{-1}$ , which signifies that the binding of NAA with  $\alpha$ -Syn was weaker as suggested by the solvophobic effect. Molecular docking further complemented the result of fluorescence binding studies and showed a moderate binding of  $-4.2 \text{ kJ}$ . The result of molecular docking also showed that NAA interacts with the glutamate residue, i.e., the hydrophilic negatively charged residue present at the C-terminal domain of  $\alpha$ -Syn. This observation of moderate binding affinity and interaction with the hydrophilic domain of  $\alpha$ -Syn may help in explaining the paradoxical effect of NAA on  $\alpha$ -Syn aggregation by the solvophobic effect.

In conclusion, this is the first study that unveils the effect of NAA on  $\alpha$ -Syn aggregation and provides caution for high concentrations of NAA in the brain. The level of NAA is different in different neurodegenerative diseases such as Canavan's disease, Alzheimer's disease, and Huntington's disease.<sup>54</sup> This ambiguity is removed by the explanation of the paradoxical effect of NAA. Still, the level of NAA in the PD condition is still not known. This study has shed light on the effect of NAA on  $\alpha$ -Syn aggregation, which may suggest researchers to measure the level of NAA in PD. Moreover, lower concentrations of NAA could be used for the therapeutic management of PD.

## ■ ASSOCIATED CONTENT

### Data Availability Statement

Data will be made available on request.

### Accession Codes

PDB: 1XQ8

## ■ AUTHOR INFORMATION

### Corresponding Authors

Anas Shamsi — Centre of Medical and Bio-allied Health Sciences Research, Ajman University, Ajman 346, United Arab Emirates; [orcid.org/0000-0001-7055-7056](https://orcid.org/0000-0001-7055-7056); Email: [anas.shamsi18@gmail.com](mailto:anas.shamsi18@gmail.com)

Asimul Islam — Centre for Interdisciplinary Research in Basic Sciences, Jamia Millia Islamia, New Delhi 110025, India; [orcid.org/0000-0001-9060-7970](https://orcid.org/0000-0001-9060-7970); Email: [aislam@jmi.ac.in](mailto:aislam@jmi.ac.in)

### Authors

Tanzeel Khan — Centre for Interdisciplinary Research in Basic Sciences, Jamia Millia Islamia, New Delhi 110025, India

Rashid Waseem — Centre for Interdisciplinary Research in Basic Sciences, Jamia Millia Islamia, New Delhi 110025, India

**Mohammad Shahid** – Department of Basic Medical Sciences, College of Medicine, Prince Sattam Bin Abdulaziz University, Al-Kharj 11942, Saudi Arabia

**Jaoud Ansari** – Centre for Interdisciplinary Research in Basic Sciences, Jamia Millia Islamia, New Delhi 110025, India; [orcid.org/0000-0002-1105-3752](https://orcid.org/0000-0002-1105-3752)

**Md. Intaiyaz Hassan** – Centre for Interdisciplinary Research in Basic Sciences, Jamia Millia Islamia, New Delhi 110025, India; [orcid.org/0000-0002-3663-4940](https://orcid.org/0000-0002-3663-4940)

Complete contact information is available at:  
<https://pubs.acs.org/10.1021/acsomega.4c00595>

## Funding

This work was supported by a grant from the Indian Council of Medical Research ISRM/12/(127)/2020.

## Notes

The authors declare no competing financial interest.

## ACKNOWLEDGMENTS

T.K. acknowledges the University Grant Commission for Junior Research Fellowship (191620050310). R.W. acknowledges the DST-INSPIRE for INSPIRE Fellowship (IF-180728). The authors are grateful to the FIST Program (SR/FST/LSI-541/2012) and Jamia Millia Islamia (a Central University) for providing infrastructural support to carry out this work. The authors acknowledge the College of Medicine and Deanship of scientific research, the Prince Sattam bin Abdul-Aziz University, Alkharj, K.S.A. for their continuous support in carrying out this research. The authors are thankful to the Ajman University for support of Ajman University Internal Research grant no. [2023-IRG-PH-4].

## REFERENCES

- (1) Balestrino, R.; Schapira, A. Parkinson disease. *European journal of neurology* **2020**, *27* (1), 27–42.
- (2) Tysnes, O.-B.; Storstein, A. Epidemiology of Parkinson's disease. *Journal of neural transmission* **2017**, *124*, 901–905.
- (3) Tanner, C. M.; Goldman, S. M. Epidemiology of Parkinson's disease. *Neurologic clinics* **1996**, *14* (2), 317–335.
- (4) Kim, W. S.; Kågedal, K.; Halliday, G. M. Alpha-synuclein biology in Lewy body diseases. *Alzheimer's Res. Ther.* **2014**, *6*, 73 DOI: [10.1186/s13195-014-0073-2](https://doi.org/10.1186/s13195-014-0073-2).
- (5) Polymeropoulos, M. H.; Lavedan, C.; Leroy, E.; Ide, S. E.; Dehejia, A.; Dutra, A.; Pike, B.; Root, H.; Rubenstein, J.; Boyer, R. Mutation in the  $\alpha$ -synuclein gene identified in families with Parkinson's disease. *Science* **1997**, *276* (5321), 2045–2047.
- (6) Clayton, D. F.; George, J. M. The synucleins: a family of proteins involved in synaptic function, plasticity, neurodegeneration and disease. *Trends in neurosciences* **1998**, *21* (6), 249–254.
- (7) Davidson, W. S.; Jonas, A.; Clayton, D. F.; George, J. M. Stabilization of  $\alpha$ -synuclein secondary structure upon binding to synthetic membranes. *J. Biol. Chem.* **1998**, *273* (16), 9443–9449.
- (8) Spillantini, M. G.; Schmidt, M. L.; Lee, V. M.-Y.; Trojanowski, J. Q.; Jakes, R.; Goedert, M.  $\alpha$ -Synuclein in Lewy bodies. *Nature* **1997**, *388* (6645), 839–840.
- (9) Baba, M.; Nakajo, S.; Tu, P.-H.; Tomita, T.; Nakaya, K.; Lee, V.; Trojanowski, J. Q.; Iwatsubo, T. Aggregation of alpha-synuclein in Lewy bodies of sporadic Parkinson's disease and dementia with Lewy bodies. *Am. J. Pathol.* **1998**, *152* (4), 879–884.
- (10) Waseem, R.; Yameen, D.; Khan, T.; Anwer, A.; Kazim, S. N.; Haque, M. M.; Hassan, M. I.; Islam, A. Aggregation of irisin and its prevention by trehalose: A biophysical approach. *J. Mol. Struct.* **2023**, *1281*, No. 135078.
- (11) Meena, V. K.; Kumar, V.; Karalia, S.; Garima; Sundd, M. Ellagic Acid Modulates Uninduced as well as Mutation and Metal-Induced Aggregation of  $\alpha$ -Synuclein: Implications for Parkinson's Disease. *ACS Chem. Neurosci.* **2021**, *12* (19), 3598–3614.
- (12) Jha, N. N.; Kumar, R.; Panigrahi, R.; Navalkar, A.; Ghosh, D.; Sahay, S.; Mondal, M.; Kumar, A.; Maji, S. K. Comparison of  $\alpha$ -synuclein fibril inhibition by four different amyloid inhibitors. *ACS Chem. Neurosci.* **2017**, *8* (12), 2722–2733.
- (13) Verma, G.; Singh, P.; Bhat, R. Disorder under stress: Role of polyol osmolytes in modulating fibrillation and aggregation of intrinsically disordered proteins. *Biophys. Chem.* **2020**, *264*, No. 106422.
- (14) Kalyal, N.; Agarwal, M.; Sen, R.; Kumar, V.; Deep, S. Paradoxical effect of trehalose on the aggregation of  $\alpha$ -synuclein: expedites onset of aggregation yet reduces fibril load. *ACS Chem. Neurosci.* **2018**, *9* (6), 1477–1491.
- (15) Beg, I.; Minton, A. P.; Hassan, M. I.; Islam, A.; Ahmad, F. Thermal stabilization of proteins by mono- and oligosaccharides: measurement and analysis in the context of an excluded volume model. *Biochemistry* **2015**, *54* (23), 3594–3603.
- (16) Ishrat, M.; Hassan, M. I.; Ahmad, F.; Islam, A. Sugar osmolytes-induced stabilization of RNase A in macromolecular crowded cellular environment. *Int. J. Biol. Macromol.* **2018**, *115*, 349–357.
- (17) Ignatova, Z.; Gierasch, L. M. Effects of osmolytes on protein folding and aggregation in cells. In *Methods in enzymology*; Elsevier, 2007; Vol. 428; pp 355–372.
- (18) Macchi, F.; Eisenkolb, M.; Kiefer, H.; Otzen, D. E. The effect of osmolytes on protein fibrillation. *International journal of molecular sciences* **2012**, *13* (3), 3801–3819.
- (19) Choudhary, S.; Kishore, N.; Hosur, R. V. Inhibition of insulin fibrillation by osmolytes: Mechanistic Insights. *Sci. Rep.* **2015**, *5* (1), 17599.
- (20) Xie, G.; Timasheff, S. N. Mechanism of the stabilization of ribonuclease A by sorbitol: preferential hydration is greater for the denatured than for the native protein. *Protein Sci.* **1997**, *6* (1), 211–221.
- (21) Chang, Y.-C.; Oas, T. G. Osmolyte-induced folding of an intrinsically disordered protein: folding mechanism in the absence of ligand. *Biochemistry* **2010**, *49* (25), 5086–5096.
- (22) Morar, A. S.; Olteanu, A.; Young, G. B.; Pielak, G. J. Solvent-induced collapse of  $\alpha$ -synuclein and acid-denatured cytochrome c. *Protein Sci.* **2001**, *10* (11), 2195–2199.
- (23) Levine, Z. A.; Larini, L.; LaPointe, N. E.; Feinstein, S. C.; Shea, J.-E. Regulation and aggregation of intrinsically disordered peptides. *Proc. Natl. Acad. Sci. U. S. A.* **2015**, *112* (9), 2758–2763.
- (24) Kaushik, J. K.; Bhat, R. Why Is Trehalose an Exceptional Protein Stabilizer?: An analysis of the thermal stability of proteins in the presence of the compatible osmolyte trehalose. *J. Biol. Chem.* **2003**, *278* (29), 26458–26465.
- (25) Kumar, R. Role of naturally occurring osmolytes in protein folding and stability. *Archives of biochemistry and biophysics* **2009**, *491* (1–2), 1–6.
- (26) Rael, L. T.; Thomas, G. W.; Bar-Or, R.; Craun, M. L.; Bar-Or, D. An anti-inflammatory role for N-acetyl aspartate in stimulated human astroglial cells. *Biochemical and biophysical research communications* **2004**, *319* (3), 847–853.
- (27) Moffett, J. R.; Ross, B.; Arun, P.; Madhavarao, C. N.; Nambodiri, A. M. N-Acetylaspartate in the CNS: from neurodiagnostics to neurobiology. *Progress in neurobiology* **2007**, *81* (2), 89–131.
- (28) Clark, J. F.; Doepke, A.; Filosa, J. A.; Wardle, R. L.; Lu, A.; Meeker, T. J.; Pyne-Geithman, G. J. N-Acetylaspartate as a reservoir for glutamate. *Medical hypotheses* **2006**, *67* (3), 506–512.
- (29) Warepam, M.; Ahmad, K.; Rahman, S.; Rahaman, H.; Kumari, K.; Singh, L. R. N-Acetylaspartate is an important brain osmolyte. *Biomolecules* **2020**, *10* (2), 286.
- (30) Waseem, R.; Khan, T.; Shamsi, A.; Shahid, M.; Kazim, S. N.; Hassan, M. I.; Islam, A. Inhibitory potential of N-acetylaspartate against protein glycation, AGEs formation and aggregation: Implication of brain osmolyte in glycation-related complications. *Int. J. Biol. Macromol.* **2023**, *244*, No. 125405.

- (31) Volles, M. J.; Lansbury, P. T. Vesicle permeabilization by protofibrillar  $\alpha$ -synuclein is sensitive to Parkinson's disease-linked mutations and occurs by a pore-like mechanism. *Biochemistry* **2002**, *41* (14), 4595–4602.
- (32) Winner, B.; Jappelli, R.; Maji, S. K.; Desplats, P. A.; Boyer, L.; Aigner, S.; Hetzer, C.; Loher, T.; Vilar, M.; Campioni, S. In vivo demonstration that  $\alpha$ -synuclein oligomers are toxic. *Proc. Natl. Acad. Sci. U. S. A.* **2011**, *108* (10), 4194–4199.
- (33) Ahanger, I. A.; Parray, Z. A.; Nasreen, K.; Ahmad, F.; Hassan, M. I.; Islam, A.; Sharma, A. Heparin accelerates the protein aggregation via the downhill polymerization mechanism: multi-spectroscopic studies to delineate the implications on proteinopathies. *ACS omega* **2021**, *6* (3), 2328–2339.
- (34) Bashir, S.; Ahanger, I. A.; Shamsi, A.; Alajmi, M. F.; Hussain, A.; Choudhry, H.; Ahmad, F.; Hassan, M. I.; Islam, A. Trehalose restrains the fibril load towards  $\alpha$ -lactalbumin aggregation and halts fibrillation in a concentration-dependent manner. *Biomolecules* **2021**, *11* (3), 414.
- (35) Kumar, S.; Kumar, R.; Kumari, M.; Kumari, R.; Saha, S.; Bhavesh, N. S.; Maiti, T. K. Ellagic acid inhibits  $\alpha$ -synuclein aggregation at multiple stages and reduces its cytotoxicity. *ACS Chem. Neurosci.* **2021**, *12* (11), 1919–1930.
- (36) Waseem, R.; Shamsi, A.; Khan, T.; Anwer, A.; Shahid, M.; Kazim, S. N.; Hassan, M. I.; Islam, A. Characterization of advanced glycation end products and aggregates of irisin: Multispectroscopic and microscopic approaches. *Journal of Cellular Biochemistry* **2023**, *124* (1), 156–168.
- (37) Ahmed, A.; Shamsi, A.; Khan, M. S.; Husain, F. M.; Bano, B. Methylglyoxal induced glycation and aggregation of human serum albumin: Biochemical and biophysical approach. *Int. J. Biol. Macromol.* **2018**, *113*, 269–276.
- (38) Shamsi, A.; Ahmed, A.; Khan, M. S.; Husain, F. M.; Bano, B. Rosmarinic acid restrains protein glycation and aggregation in human serum albumin: multi spectroscopic and microscopic insight-possible therapeutics targeting diseases. *Int. J. Biol. Macromol.* **2020**, *161*, 187–193.
- (39) Waseem, R.; Yadav, N. S.; Khan, T.; Ahmad, F.; Kazim, S. N.; Hassan, M. I.; Prakash, A.; Islam, A. Molecular basis of structural stability of Irisin: A combined molecular dynamics simulation and in vitro studies for Urea-induced denaturation. *J. Mol. Liq.* **2023**, *372*, No. 121120.
- (40) Ahanger, I. A.; Bashir, S.; Parray, Z. A.; Alajmi, M. F.; Hussain, A.; Ahmad, F.; Hassan, M. I.; Islam, A.; Sharma, A. Rationalizing the role of monosodium glutamate in the protein aggregation through biophysical approaches: Potential impact on neurodegeneration. *Frontiers in neuroscience* **2021**, *15*, No. 636454.
- (41) Shamsi, A.; Shahwan, M.; Khan, M. S.; Husain, F. M.; Alhumaydhi, F. A.; Aljohani, A. S.; Rehman, M. T.; Hassan, M. I.; Islam, A. Elucidating the interaction of human ferritin with quercetin and naringenin: Implication of natural products in neurodegenerative diseases: Molecular docking and dynamics simulation insight. *ACS omega* **2021**, *6* (11), 7922–7930.
- (42) Lakowicz, J. R. *Principles of fluorescence spectroscopy*; Springer, 2006.
- (43) Feng, X.-Z.; Lin, Z.; Yang, L.-J.; Wang, C.; Bai, C.-I. Investigation of the interaction between acridine orange and bovine serum albumin. *Talanta* **1998**, *47* (5), 1223–1229.
- (44) Batzli, K. M.; Love, B. J. Agitation of amyloid proteins to speed aggregation measured by ThT fluorescence: a call for standardization. *Materials Science and Engineering: C* **2015**, *48*, 359–364.
- (45) Brahma, A.; De, D.; Bhattacharyya, D. Rayleigh scattering technique as a method to study protein–protein interaction using spectrofluorimeters. *Curr. Sci.* **2009**, 940–946.
- (46) Khan, A. N.; Hassan, M. N.; Khan, R. H. Gallic acid: A naturally occurring bifunctional inhibitor of amyloid and metal induced aggregation with possible implication in metal-based therapy. *J. Mol. Liq.* **2019**, *285*, 27–37.
- (47) Waseem, R.; Anwar, S.; Khan, S.; Shamsi, A.; Hassan, M. I.; Anjum, F.; Shafie, A.; Islam, A.; Yadav, D. K. MAP/Microtubule affinity regulating kinase 4 inhibitory potential of Irisin: A new therapeutic strategy to combat cancer and Alzheimer's Disease. *International journal of molecular sciences* **2021**, *22* (20), 10986.
- (48) Waseem, R.; Shamsi, A.; Khan, T.; Hassan, M. I.; Kazim, S. N.; Shahid, M.; Islam, A. Unraveling the binding mechanism of Alzheimer's Drugs with irisin: Spectroscopic, calorimetric, and computational approaches. *International journal of molecular sciences* **2022**, *23* (11), 5965.
- (49) Shamsi, A.; Mohammad, T.; Anwar, S.; AlAjmi, M. F.; Hussain, A.; Rehman, M. T.; Islam, A.; Hassan, M. I. Glecaprevir and Maraviroc are high-affinity inhibitors of SARS-CoV-2 main protease: possible implication in COVID-19 therapy. *Biosci. Rep.* **2020**, *40* (6), No. BSR20201256.
- (50) Shamsi, A.; Ahmed, A.; Khan, M. S.; Husain, F. M.; Amani, S.; Bano, B. Investigating the interaction of anticancer drug temsirolimus with human transferrin: Molecular docking and spectroscopic approach. *J. Mol. Recognit.* **2018**, *31* (10), No. e2728.
- (51) Kalia, L. V.; Lang, A. E. Parkinson's disease. *Lancet* **2015**, *386* (9996), 896–912.
- (52) Rabbani, G.; Choi, I. Roles of osmolytes in protein folding and aggregation in cells and their biotechnological applications. *Int. J. Biol. Macromol.* **2018**, *109*, 483–491.
- (53) Roy, S.; Bhat, R. Effect of polyols on the structure and aggregation of recombinant human  $\gamma$ -Synuclein, an intrinsically disordered protein. *Biochimica et Biophysica Acta (BBA)-Proteins and Proteomics* **2018**, *1866* (10), 1029–1042.
- (54) Tsai, G.; Coyle, J. T. N-acetylaspartate in neuropsychiatric disorders. *Progress in neurobiology* **1995**, *46* (5), 531–540.